Grazing Reflectivity of the Wind-Ruffled Sea

C. R. Zeisse

SSC San Diego

20010109 063

SPAWAR
Systems Center
San Diego

TECHNICAL REPORT 1843
October 2000

Grazing Reflectivity of the Wind-Ruffled Sea

C. R. Zeisse

**SPAWAR
Systems Center
San Diego**

SSC San Diego
San Diego, CA 92152-5001

DTIC QUALITY INSPECTED 3

SSC SAN DIEGO
San Diego, California 92152-5001

Ernest L. Valdes, CAPT, USN
Commanding Officer

R. C. Kolb
Executive Director

ADMINISTRATIVE INFORMATION

The work described in this report was performed for the Office of Naval Research by the SSC San Diego Atmospheric Propagation Branch (D858).

Released by
R. A. Paulus, Head
Atmospheric Propagation Branch

Under authority of
C. J. Sayre, Head
Electromagnetics &
Advanced Technology
Division

SB

EXECUTIVE SUMMARY

OBJECTIVE

The objective of this study was to determine the grazing optical reflectivity of an ocean covered by capillary waves.

APPROACH

Starting with an integral equation for ocean reflectivity, we introduced approximations applicable in the grazing regime and arrived at an analytic formula for the grazing ocean reflectivity of circular sources such as the Sun.

RESULT

The analytic approximation depends on the variance of the capillary wave slopes, the angular radius of the source, and the grazing angles of the source and receiver.

Preceding Page Blank

CONTENTS

Figures

Tables

1. INTRODUCTION

The reflection of distant objects in the sky by the rough sea surface produces interesting natural effects. Several thoughtful observers have commented on these effects. Minnaert (1954) says, "The first 25° or 35° of the sky above the horizon are, in reality, hardly visible in the reflection. [This phenomenon is] easily explained; at a great distance we can only see the sides of the waves turned towards us. This makes it seem as if we saw all the objects in the sky reflected in a slanting mirror." Cox and Munk (1955) pointed out that "If the sea were absolutely flat, then the radiance of the sea surface just beneath the horizon would equal the radiance of the sky just above it, and there would be no visible horizon." In other words, the fact that we see the ocean horizon is proof that the sea is rough. Shaw (1999) recently re-emphasized that the width of a sun glint pattern is a sensitive measure of the wind speed directly above that pattern. All these comments refer to a grazing geometry when the source and receiver are at relatively low altitudes, say several tens of meters, but are separated by a range of several tens of kilometers. This report presents an approximate formula for the grazing reflection of a circular source by the rough sea. The formula can be applied, for example, to the reflectivity along the center of a sun glint pattern or to the reflectivity of a missile plume (considered as a circle) as seen from the deck of a ship.

In the optical region, the reflectivity of an ocean without gravity waves can be calculated using geometrical optics. The reason is that the wavelength of the radiation being reflected is much less than the radius of curvature of a typical capillary wave facet. The ocean can therefore be modeled as a collection of flat, mirror-like facets whose tilts fluctuate at random under the wind's influence. If the slope of a facet is correct, a ray from a source such as the Sun will be reflected into an optical receiver such as the eye. The problem then reduces to finding the Fresnel reflectivity of a small seawater mirror and counting the relative number of mirrors which, on average, can reflect a ray from the source into the receiver.

Of course, Cox and Munk (1954, 1955, and 1956) have already addressed this problem in a famous series of papers. They measured the statistical occurrence of various capillary wave slopes by taking photographs of sun glitter from an airplane. However, their equation for reflected radiance applies to the case where the ocean is observed from above, not to the grazing case. When calculating reflectivity, Cox and Munk assumed that a patch of ocean of area A appears to have an area of $A \sin\Psi$ when viewed from the side at a grazing angle, Ψ. In other words, for that part of their calculation, they assumed that the patch was flat. Because radiance involves the power received per unit solid angle per unit projected area, and because the projected area of an ideal flat surface approaches zero at a grazing angle of observation, the radiance obtained by Cox and Munk approaches infinity at grazing. Even so, their analysis is quite good for those elevations greater than about 10°. For observations at elevations less than 10°, especially for those approaching 0°, their approach must be modified by using the fact that the sea is a rough surface that can be seen even at very small grazing angles.

It is interesting to compare the results already obtained by the radar community for the grazing reflectivity of the rough ocean surface. Radar wavelengths fall in the range of 1 mm to 1 cm, and a typical radar footprint (Kerr, Fishback, and Goldstein, 1951) (given by the size of the first Fresnel zone) is about 1 km along the propagation direction and 10 m perpendicular to it. The basic radar reflection model (Ament, 1953) assumes that the ocean is covered by gravity waves alone. With this assumption, geometrical optics can be used for radar because the radar wavelength is much less than the wavelength of an ocean gravity wave. The sinusoidal gravity wave is approximated by a series of horizontal sections and a specular reflection is assumed to occur at each section. Each horizontal

1

section with altitude, y, introduces a phase shift, $4\pi\, y \sin \Psi/\lambda$, compared to the reflection, Γ_o, from the smooth surface at $y = 0$ (mean sea level). After superimposing gravity waves at various wavelengths, the sections are assumed to have an altitude that is randomly distributed according to a Gaussian law about mean sea level. The total rough surface reflectivity, Γ, is found by integrating over all possible altitudes with the result, for radar, that

$$\frac{\Gamma}{\Gamma_o} \equiv \rho = \exp\left(-g^2/2\right),$$

$$g \equiv 4\pi\ \sigma_h \sin \Psi/\lambda,$$

(1)

where σ_h is the standard deviation of the gravity wave altitude distribution. This result underestimated measurements of very rough surfaces and was improved by assuming that the gravity waves not only had a Gaussian amplitude distribution, but also a uniform phase distribution (Miller, Brown, and Vegh, 1984).

These considerations for radar apply only to so-called coherent (specular) reflection; there is also a diffusely reflected (scattered) component. A recent review of radar rough surface reflectivity (Barrick, 1998) notes that propagation and scattering are "inextricably connected" at grazing and that their improper separation has led to contradictions in associating theory with experiment.

From my point of view, the primary distinction between radar reflectivity and optical reflectivity is this: For radar reflectivity one assumes that local regions of the reflecting surface are horizontal whereas for optical reflectivity one assumes that local regions are tilted. When coupled with the fact that the Fresnel reflectivity of any smooth surface approaches 100% at grazing, this results in qualitatively different behavior for grazing reflectivity of rough radar and rough optical surfaces. In the most coarse approximation, the radar sea is nominally flat and the reflectivity at exact grazing ($\Psi = 0$) is close to 100% whereas the optical sea is mostly tilted and the reflectivity at exact grazing is close to 0%.

2. OCEAN REFLECTIVITY

Projection of a rough surface toward the observer and the neglect of gravity waves are important aspects of the optical description of ocean reflectivity. The second aspect is a severe restriction. Gravity waves significantly influence the tilt of all capillary wave facets and, hence, significantly influence the reflectivity. Furthermore, I do not consider shadowing or multiple reflections, two effects that become increasingly important as exact grazing is approached. Therefore, I will be content with a rough form for grazing reflectivity, perhaps good to within only a factor of two for larger sources such as the Sun at lower wind speeds such as ¼ m s^{-1}.

Let Γ be the optical reflectivity of the rough ocean surface. This means that when a radiance, N_o, is incident on the ocean surface, the reflected radiance, N_r, will be given by ΓN_o. The following pair of equations (Zeisse, 1995) gives a rough surface reflectivity that is the mathematically exact consequence of the physical approximations mentioned in the previous paragraph:

$$\Gamma = \frac{N_r}{N_o} = \iint_{\substack{ellipse \\ U_r=const}} \Gamma_o \, q_r \, d\zeta_x d\zeta_y \tag{1}$$

$$q_r = \frac{(\cos\omega \, \cos\theta_n)p}{\displaystyle\iint_{\substack{\omega \leq \pi 2 \\ U_r=const}} (\cos\omega \, \cos\theta_n)p \, d\zeta_x d\zeta_y} . \tag{2}$$

In these equations, ω is the angle of incidence for a specular reflection between source and receiver at a capillary wave facet, $\Gamma_o (\omega, \lambda)$ is the smooth surface reflectivity of seawater at ω and optical wavelength, λ, θ_n is the zenith angle of the facet normal (also known as the facet tilt), and ζ_x and ζ_y are the facet slopes in the upwind and crosswind directions, respectively. The function, $p(\zeta_x, \zeta_y, W)$, is the well-known Cox-Munk wave slope probability density,

$$p \approx \frac{1}{2\pi\sigma_u\sigma_c} \exp\left[-\frac{1}{2}\left(\frac{\zeta_x^2}{\sigma_u^2} + \frac{\zeta_y^2}{\sigma_c^2}\right)\right]$$

$$\sigma_u^2 = 0.000 + 3.16\times10^{-3}W \tag{3}$$

$$\sigma_c^2 = 0.003 + 1.92\times10^{-3}W$$

which has the shape of a two-dimensional bell in slope space. In equation (3), σ_u^2 and σ_c^2 are the facet slope variances in the upwind and crosswind directions, respectively, and W is the wind speed in m s^{-1}. The quantity $p(\zeta_x, \zeta_y, W) \, d\zeta_x d\zeta_y$ gives the probability that a wave facet will have a slope within $\pm$ $d\zeta_x/2$ of ζ_x and $\pm d\zeta_y/2$ of ζ_y when the wind speed is W. This quantity can also be interpreted as the fractional area within the footprint occupied by all facets whose slope falls within the specified range.

The function q_r embodies the assumption, first put forward by Plass, Kattawar, and Guinn (1975), that the importance of a particular facet within a wind-ruffled ocean footprint is given by the area of that facet projected toward the receiver. For a single facet whose slope is (ζ_x, ζ_y), this projection is accomplished by the factor $(\cos\omega/\cos\theta_n)$ in equation (2). Therefore, the denominator of q_r represents the area of all facets projected toward the receiver, which is the same as the projected area of the entire footprint considered as a rough surface. When performing the integral in the

denominator of q_r, the notations under the integral signs serve as a reminder that (1) the angle of incidence must remain less than 90°, and (2) receiver coordinates are held fixed during the integration. The first restriction means that only the front of each facet is used to evaluate the integral because, as Minnaert (1954) says, "at a great distance we can only see the sides of the waves turned towards us."

Finally, the word "ellipse" under the integral in equation (1) means that the integral is confined to slopes within the tolerance ellipse[1]. The area of the tolerance ellipse is

$$E = \iint\limits_{ellipse} d\zeta_x d\zeta_y \approx \left\{ \frac{\sec\omega \sec^3\theta_n}{4} \right\} \pi\varepsilon^2 , \tag{4}$$

where ε is the angular radius of the source subtended at the ocean footprint. The approximation made in equation (4) is that the quantities inside the bracket, namely, the angle of incidence and the facet tilt, remain constant as the ray from the source varies across the disk.

Equations (1) and (2) apply at all receiver elevations, but they are obscure. Fortunately, at receiver elevations greater than about 10° they reduce to the simple form used by Cox and Munk (1954, 1955, and 1956). In the grazing regime equations (1) and (2) must still be used and there they must be numerically evaluated. In this report, I derive a more easily evaluated approximate form.

---

[1] When there is a specular reflection at the facet from the sky to a receiver whose position is held fixed, the law of reflection can be used to associate a sky location with an ocean slope. By considering the Jacobian of the transformation from ocean slopes to a coordinate system centered on a circular source in the sky, such as the Sun, it can be shown that a disk in the sky is associated with an elliptical region of slope space. Cox and Munk called this region the "tolerance ellipse."

3. GRAZING OCEAN REFLECTIVITY

Consider a receiver (such as a camera in the infrared or an eye in the visible) observing a distant circular source (such as the Sun or the mirror of a telescope transmitter). Imagine that the camera is mounted on a ship, or the observer is on the shore, while the source is near the horizon in the distant sky. Figure 1 shows the geometry for this situation, where Ψ_s and Ψ_r are the source and receiver elevations, respectively. I chose a coordinate system[2] that has an origin at the point of reflection, with the Z-axis pointing to the zenith, the Y-axis pointing to the center of the source, and the X-axis such that a right-handed system is formed. Let U be a unit vector with coordinates (a, b, c) in this system.
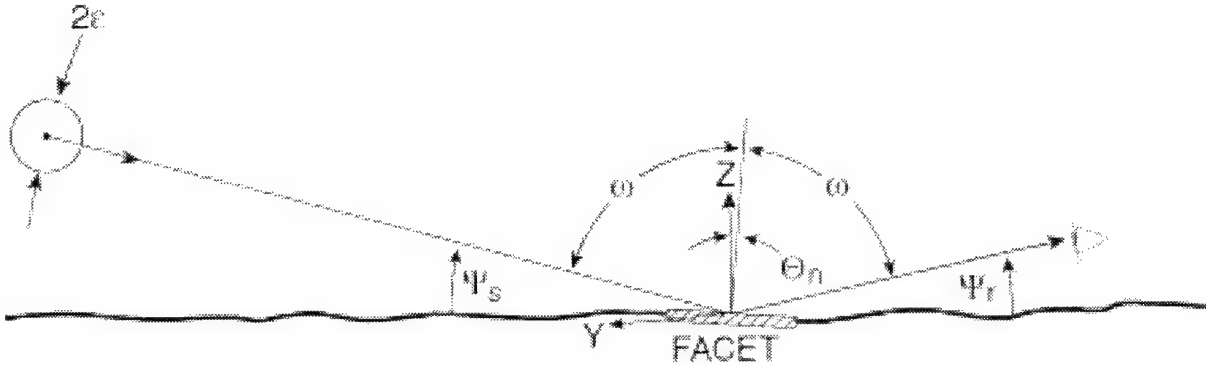

Figure 1. Grazing geometry for capillary wave reflectivity. A specular reflection occurs at the flat capillary wave facet that is tilted with respect to the zenith direction by the angle, θ_n. The source, assumed to be circular, has an angular radius of ε. The facet is shown with a positive slope in the Y direction.

The law of reflection provides the following relationships among the angles in figure 1:

$$\omega = \frac{\pi}{2} - \frac{\Psi_r + \Psi_s}{2} \equiv \frac{\pi}{2} - \Psi$$

$$\theta_n = \frac{\Psi_s - \Psi_r}{2}$$

(5)

where Ψ is the average grazing angle of the source and receiver. Typical values for grazing angles can be obtained from the following considerations. The height of the receiver may vary from several tens of meters (for a camera mounted on a ship) to several meters (for a human). In either case, the range from the receiver to the ocean footprint will vary from several km to several tens of km. The elevation of the center of the source may vary from a minimum when the limb of the source just touches the geometrical horizon to an arbitrary maximum of about 100 mrad (5.73°). Hence, the grazing angles will fall in the following ranges for the case when the source is the Sun:

$$1 \text{ mrad} \leq \Psi_r \leq 10 \text{ mrad}$$

$$4 \text{ mrad} \leq \Psi_s \leq 100 \text{ mrad}$$

(6)

---

[2] In previous equations, here, and in Zeisse (1995) and Cox and Munk (1954, 1956), the X-axis pointed in the upwind direction.

From this point on, I assume that the receiver is looking directly toward the source, as figure 1 shows, and I consider grazing angles in the ranges given by equation (6). I also assume that the source is the Sun, although the derivation applies to a circular source of any radius up to and including the Sun's radius (4.641 mrad).

Figure 2, reprinted from Zeisse (1995), shows how q_r depends on slope when the wind speed is 10 m s^{-1} and the ray propagating towards the receiver leaves the footprint at the grazing angle of ¼°. The dark regions shown on the surface of q_r are the tops of a parade of sun glint columns for seven different positions of the Sun. A sun glint column is that portion of slope space over the tolerance ellipse and under the function, $\Gamma_o q_r$. The entire volume under $\Gamma_o q_r$ is unity according to equation (2), and the volume of a glint column is, according to equation (1), the rough surface reflectivity I seek.
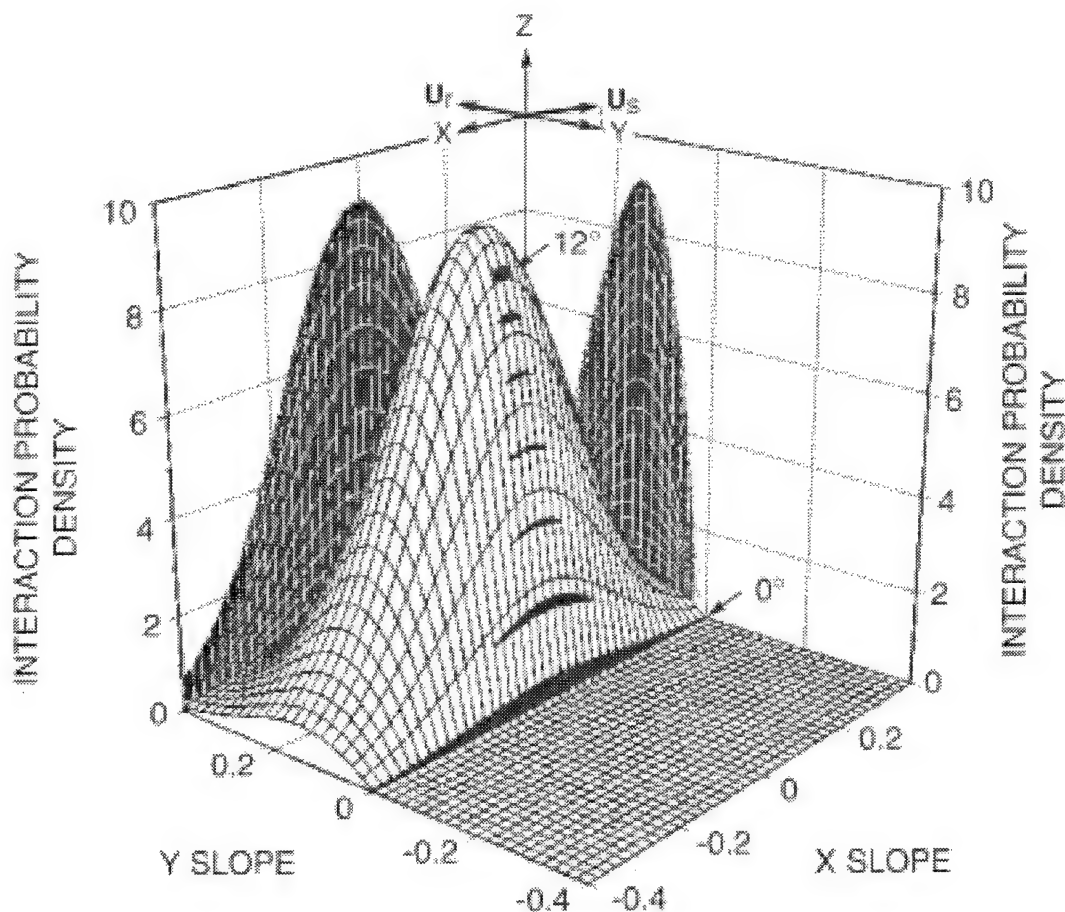

Figure 2. Plass-Cox-Munk interaction probability density, q_r, for a wind speed of 10 m s^{-1} and a receiver elevated by 4.4 mrad (1/4°). The receiver looks directly toward the Sun. The figure is drawn for a smooth surface reflectivity of unity. Each dark area represents the top of a sun glint column for solar elevations increasing from 0 to 210 mrad (0° to 12°) in equal steps of 35 mrad (2°).

4. SMOOTH OCEAN REFLECTIVITY

Figure 3 shows the smooth surface reflectivity of seawater. The unpolarized values are the average of the two polarized values, "S" for radiance polarized normal to the plane of incidence, and "P" for radiance polarized parallel to the plane of incidence. The circles are the result of an exact calculation (Stratton, 1941) for the Fresnel reflectivity of a medium with the complex optical index (Hale and Querry, 1973[3]; Querry et al., 1977[4]) of seawater. The lines for the polarized data in figure 3 are an exponential fit that is forced to go between 1 at an elevation of zero and the exact value at an elevation of 100 mrad. The line for the unpolarized data is the average of the other two lines. That is,

$$R_{os}(\Psi, \lambda) = \exp[-b_s(\lambda)\Psi]$$
$$R_{op}(\Psi, \lambda) = \exp[-b_p(\lambda)\Psi]$$
$$R_o(\Psi, \lambda) = \{R_{os}(\Psi, \lambda) + R_{op}(\Psi, \lambda)\}/2 \tag{7}$$
$$b_s \equiv -10 \times \ln \Gamma_{os}(0.1, \lambda)$$
$$b_p \equiv -10 \times \ln \Gamma_{op}(0.1, \lambda)$$

where $\Gamma_o(\Psi, \lambda)$ is the calculated value and $R_o(\Psi, \lambda)$ is the fitted value. (I have used equation (5) to replace the angle of incidence with the grazing angle in these arguments.) For wavelengths between 0.4 and 12 μm, and elevations between 0 and 100 mrad, the maximum absolute error between the calculation and the fit is 0.0016. This maximum error occurs at the wavelength of 3.2 μm used for figure 3. Figure 4 shows how the Fresnel reflectivity depends on wavelength and table 1 lists the value of the constants, b_s and b_p, as a function of wavelength.

---

[3] These data, for pure water, were used from 0.2 to 2 μm.
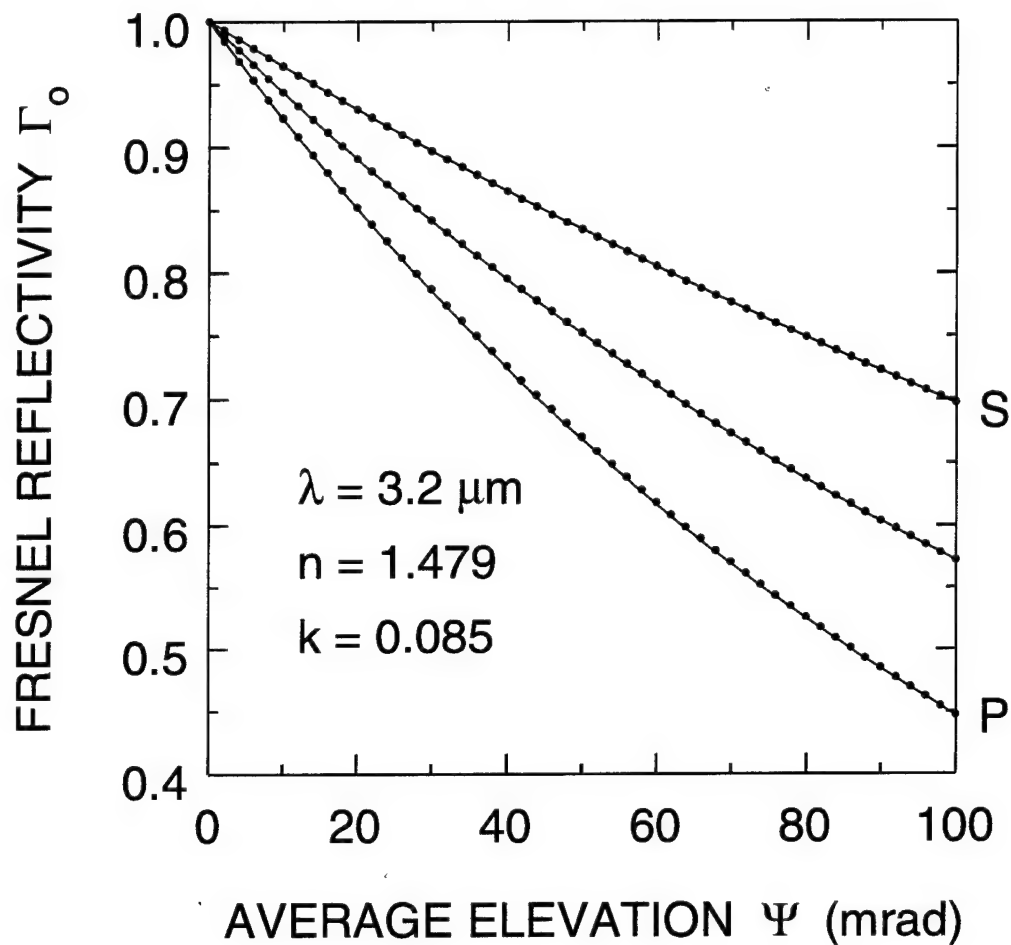
[4] These data, for seawater, were used from 2.2 to 12 μm.

Figure 3. Smooth surface reflectivity of seawater as a function of average elevation for an optical wavelength of 3.2 μm. Circles are the result of an exact calculation and lines show an exponential fit given by equation (7). The data labeled "S" are for radiance polarized perpendicular to the plane of incidence, the data labeled "P" are for radiance polarized parallel to the plane of incidence, and the unlabeled data are for unpolarized radiance.
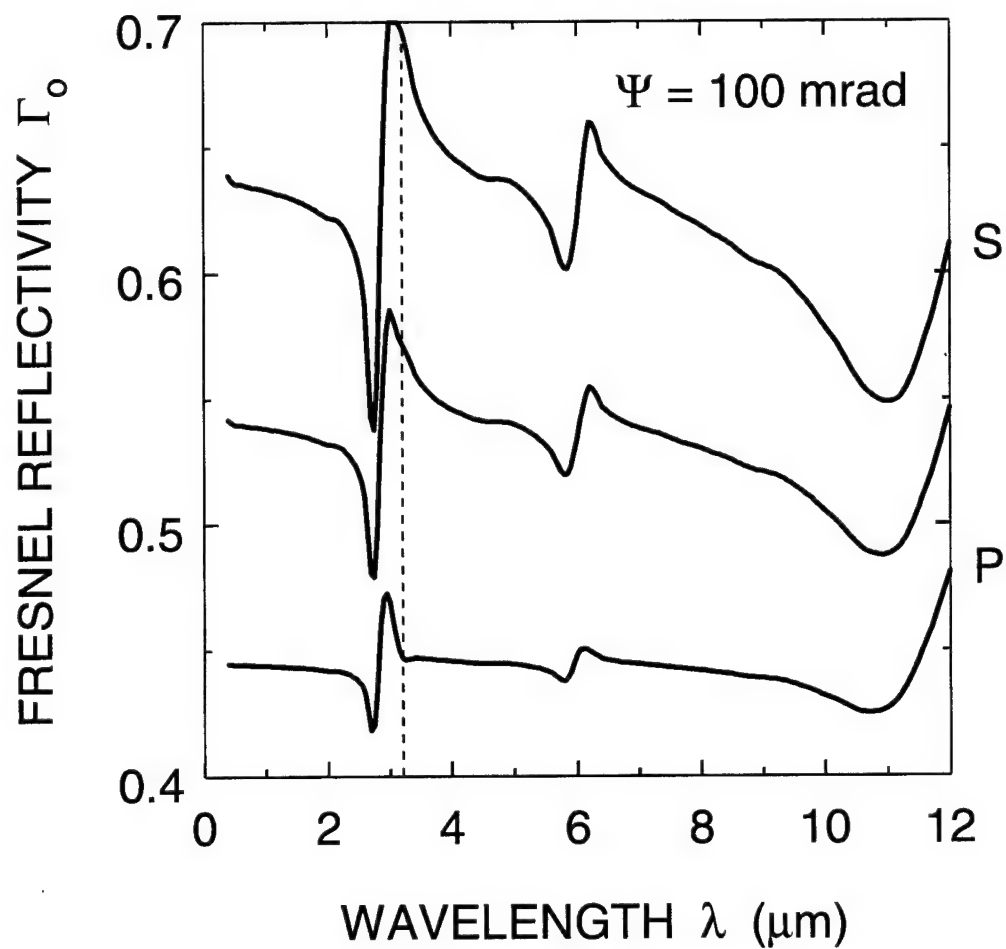
8

Figure 4. Smooth surface reflectivity of seawater as a function of optical wavelength for an average elevation of 100 mrad. The curves have the same meaning as those given in the previous figure. The vertical dashed line indicates the wavelength used in figure 3.

Table 1. Fresnel reflectivity of seawater at an average grazing angle of 100 mrad. The constants, b_s and b_p, are defined in equation (7).

λ (μm)	b_s	b_p
0.4	4.48	8.10
0.6	4.53	8.11
0.8	4.55	8.11
1.0	4.55	8.11
1.2	4.59	8.12
1.4	4.62	8.13
1.6	4.65	8.14
1.8	4.69	8.15
2.0	4.74	8.16
2.2	4.77	8.17
2.4	4.92	8.22
2.6	5.30	8.36
2.8	5.86	8.31
3.0	3.54	7.56
3.2	3.61	8.05
3.4	3.95	8.05
3.6	4.14	8.06
3.8	4.27	8.07
4.0	4.36	8.08
4.2	4.41	8.09
4.4	4.47	8.10
4.6	4.47	8.10
4.8	4.50	8.10
5.0	4.53	8.11
5.2	4.59	8.12
5.4	4.69	8.15
5.6	4.83	8.19
5.8	5.08	8.26
6.0	4.78	8.02
6.2	4.16	7.99
6.4	4.34	8.06
6.6	4.45	8.08
6.8	4.53	8.10
7.0	4.57	8.11
7.2	4.61	8.12
7.4	4.66	8.13
7.6	4.71	8.14
7.8	4.76	8.16
8.0	4.80	8.17
8.2	4.85	8.18
8.4	4.90	8.19
8.6	4.96	8.21
8.8	5.02	8.23
9.0	5.05	8.24
9.2	5.09	8.25
9.4	5.15	8.27
9.6	5.25	8.31
9.8	5.34	8.35

Table 1. Fresnel reflectivity of seawater at an average grazing angle of 100 mrad. The constants, b_s and b_p, are defined in equation (7). (continued)

λ (μm)	b_s	b_p
10.0	5.47	8.40
10.2	5.59	8.44
10.4	5.74	8.50
10.6	5.88	8.55
10.8	5.97	8.55
11.0	6.00	8.51
11.2	5.96	8.40
11.4	5.80	8.20
11.6	5.55	7.93
11.8	5.26	7.64
12.0	4.92	7.32

5. ROUGH OCEAN REFLECTIVITY

In this section (and the appendix), I introduce approximations into equations (1) and (2) that reduce them to an easily evaluated algebraic form. The final approximate form, equation (14), depends only on the grazing angles, the source radius, and the wind speed.

The first simplification eliminates the distinction between upwind and crosswind slope variances. I replace each of these with their arithmetic mean value:

$$\sigma^2 \equiv \frac{\sigma_c^2 + \sigma_u^2}{2} \tag{8}$$

$$= 0.0015 + 2.54 \times 10^{-3} \, W \, .$$

One standard deviation, containing 90% of all wave slopes, corresponds to a tilt of $\theta_n = \tan^{-1}\sigma \approx$ 64 mrad (3 2/3 °), at a wind speed of 1 m s^{-1} or 163 mrad (9 1/3 °) at a wind speed of 10 m s^{-1}.

After making this change and inserting equations (2) and (3) into equation (1), the reflectivity is

$$\Gamma = \frac{A}{B_r} \frac{1}{2\pi} \iint_{\substack{ellipse \\ U_r = const}} \Gamma_o \cos\omega \, \sec\theta_n \, \exp\{-(u^2 + v^2)/2\} du \, dv \, , \tag{9}$$

where the variables of integration are

$$u \equiv \zeta_x / \sigma$$
$$v \equiv \zeta_y / \sigma \, . \tag{10}$$

I have also replaced the denominator of equation (2) by its geometrical representation, B_r/A, where A is the footprint area in the plane of mean sea level and B_r is the area (projected towards the receiver) of the rough sea surface above that footprint. During the integration of equation (9), the receiver ray stays fixed while the source ray varies systematically across the Sun with the facet tilt adjusting itself to maintain a specular reflection.

To understand the behavior of equation (9), we must understand how the tolerance ellipse appears in slope space during grazing. Figure 5 shows how the shape of the tolerance ellipse depends on solar elevation when the receiver is elevated by 1 mrad. An estimate of a, the semi-major axis of the tolerance ellipse, may be obtained from an estimate of the semi-minor axis b and approximate area of the ellipse given by equation (4):

$$b \approx \frac{\varepsilon}{2}$$

$$a = \frac{E}{\pi b} \approx \frac{\sec\omega\sec^3\theta_n \, \varepsilon}{2} \approx \frac{\varepsilon}{2\Psi} \tag{11}$$

When the lower limb of the Sun just touches the geometrical horizon, and for the receiver at exact grazing ($\Psi_r = 0$), $\Psi = \Psi_s / 2 = \varepsilon / 2$ and equation (11) shows that $a \approx 1$, corresponding to a tilt of 45°. At grazing, the tolerance ellipse has become very large in the X-direction, so large that the trigonometric terms in equation (9) vary considerably from their value at the center of the ellipse. Nevertheless, I may remove these terms, and Γ_o as well, from the integral in equation (9) without

13

appreciable error because these terms vary slowly across the ellipse compared to the rapid fall-off of the exponential term away from the center. After removing them, replacing them by their central value, and then applying the small angle approximation to the central value, equation (9) becomes

$$\Gamma \approx \frac{A}{B_r} \frac{\Gamma_o \Psi}{2\pi} \iint\limits_{\substack{ellipse \\ U_r=const}} \exp\{-(u^2 + v^2)/2\} du\, dv . \qquad (12)$$

Next, I replace the ellipse by the rectangle that just contains it and introduce a factor of $\pi/4$ to take into account the different areas of these two shapes:

$$
\begin{aligned}
\Gamma &\approx \frac{A}{B_r} \frac{\Gamma_o \Psi}{2\pi} \frac{\pi}{4} \int_{-a\,\sigma}^{+a\,\sigma} du\, \exp(-u^2/2) \int_{-b\,\sigma}^{+b\,\sigma} dv\, \exp(-v^2/2) \\
&\approx \frac{A}{B_r} \frac{\Gamma_o \Psi}{8} 2\pi\ erf\!\left(\frac{a}{\sqrt{2}\sigma}\right) erf\!\left(\frac{b}{\sqrt{2}\sigma}\right) \qquad (13) \\
&\approx \sqrt{2\pi}\, \frac{A}{B_r} \Gamma_o \Psi \frac{\varepsilon}{8\sigma}\ erf\!\left(\frac{\varepsilon}{2\sqrt{2}\,\sigma\,\Psi}\right)
\end{aligned}
$$

In equation (13), the error function involving b has been approximated for small values of its argument and equation (11) has been used to eliminate the semi-major axis of the tolerance ellipse.
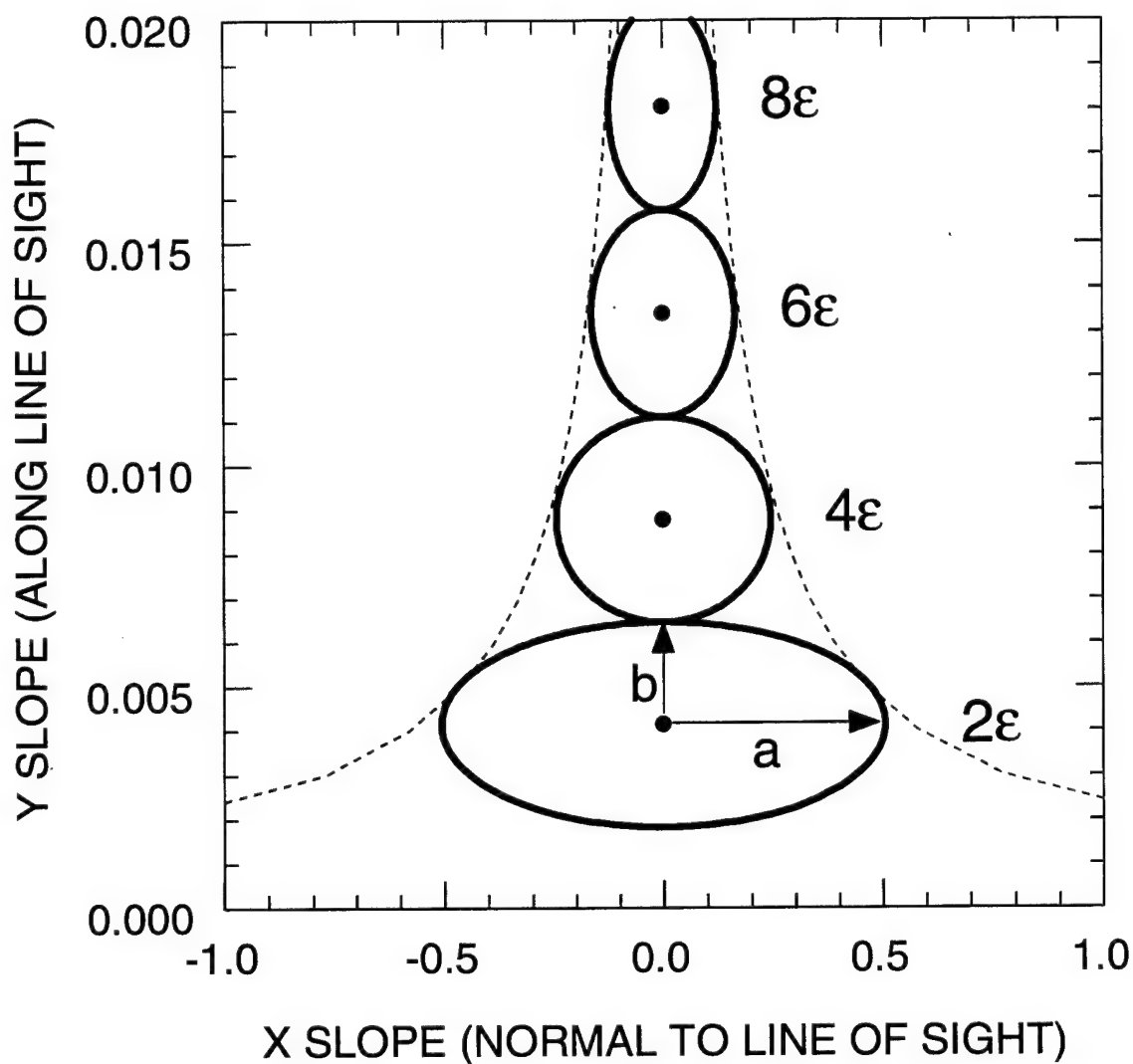
Figure 5. A sequence of tolerance ellipses for the rising (or setting) Sun. The receiver is looking directly toward the Sun from an elevation of 1 mrad. The parameter next to each ellipse is the elevation of the solar center in terms of the solar radius, ε. The dashed line shows the approximation for the semi-major axis of the ellipse given by equation (11).

6. FINAL RESULT

Combining equation (13) with the result given in appendix A for the quantity, B_r/A, I obtain the following expression for the grazing reflectivity of a circular source:

$$\frac{\Gamma}{\Gamma_o} \equiv \rho \approx \frac{\pi}{4}\frac{\varepsilon}{\sigma}\frac{\Psi}{\sigma}\frac{1}{f(\Psi, \sigma)}\ erf\ \left(\frac{\varepsilon}{2\sqrt{2}\ \sigma\ \Psi}\right)$$

$$f(x) \approx 1 + \sqrt{\frac{\pi}{2}}\ x + \frac{x^2}{2} - \frac{7}{24}x^4 + ...$$

(14)

Figures 6 and 7 present a comparison of equation (14) with the numerical evaluation of equations (1) and (2) for wind speeds of 10 and ¼ m s⁻¹, respectively.
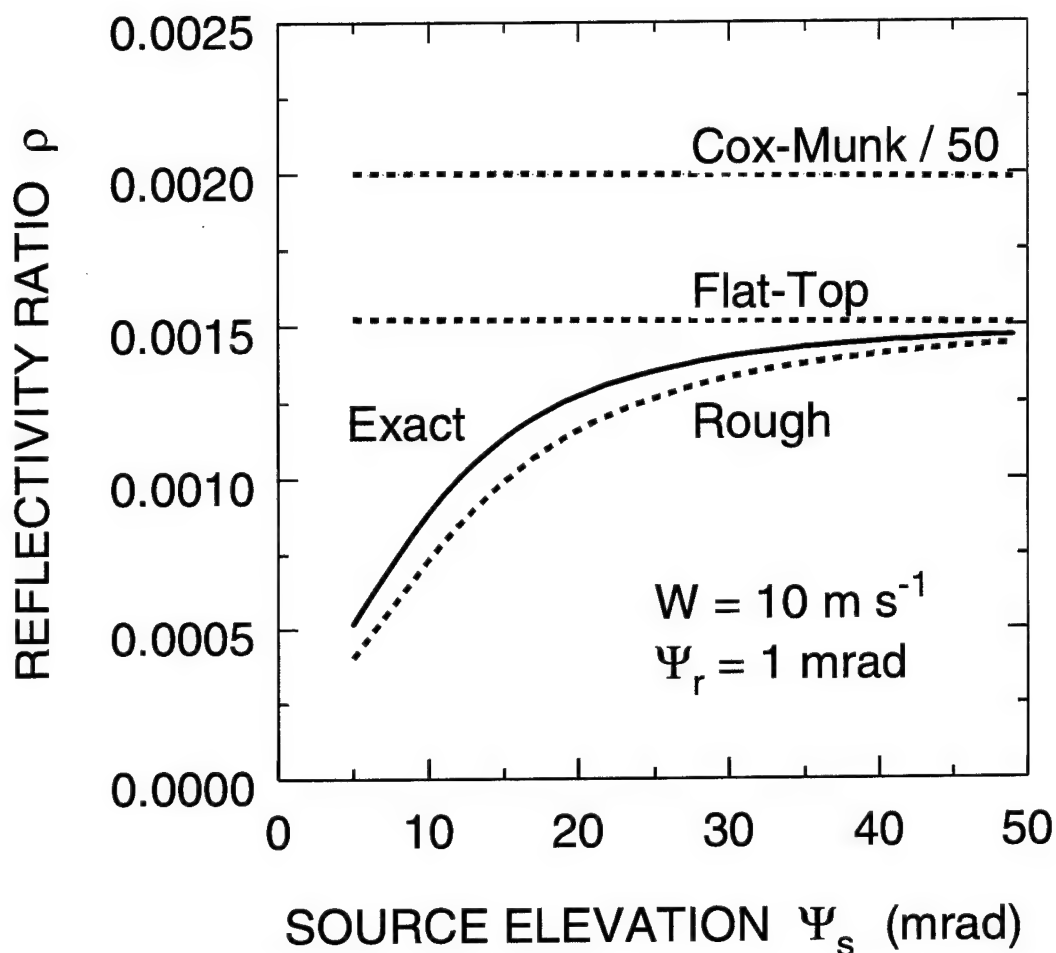
Figure 6. Rough ocean reflectivity as a function of solar elevation. The receiver is elevated by 1 mrad and the wind speed is 10 m s^{-1}. The solid line labeled "Exact" is a numerical calculation based on equations (1) and (2). The dashed line labeled "Rough" is equation (14). The dashed line labeled "Flat-Top" is equation (23) of Zeisse (1995). The dashed line labeled "Cox-Munk/50" is equation (9) of Cox and Munk (1954) after division by a factor of 50.
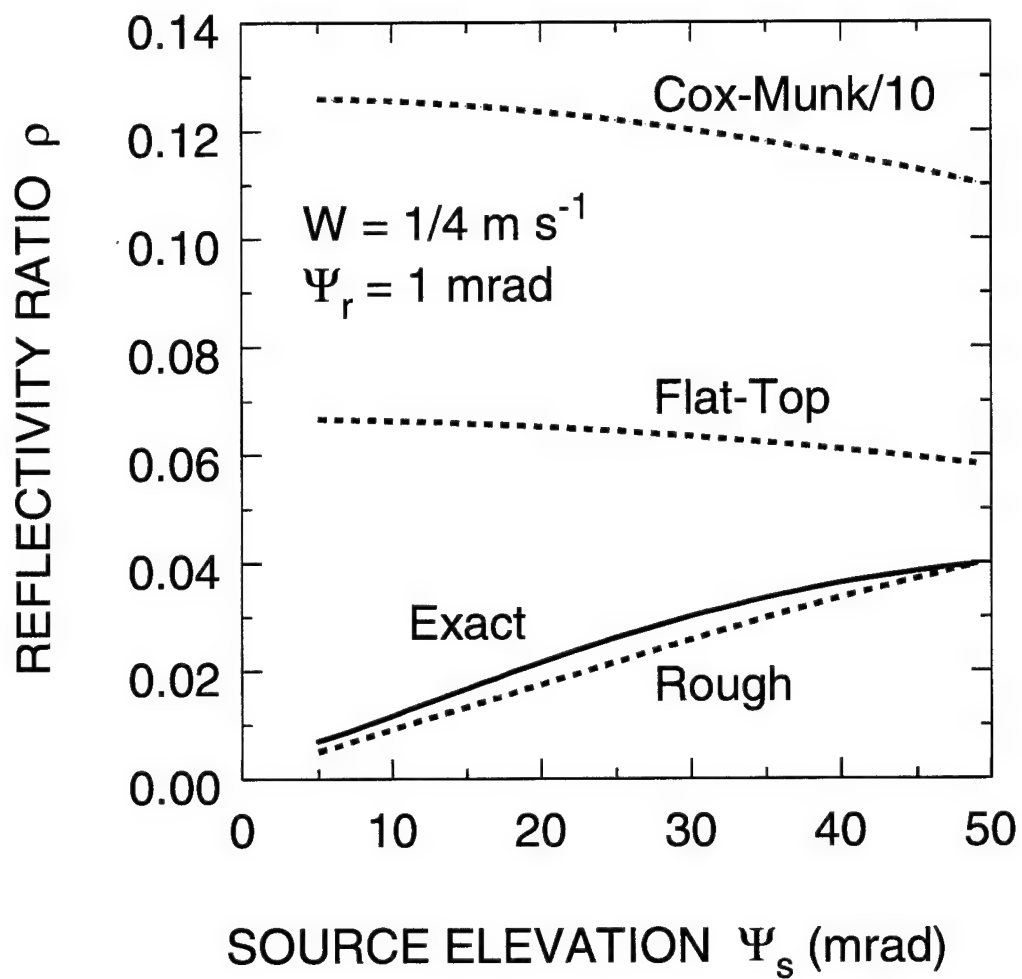
18

Figure 7. The same as figure 6 for a wind speed of ¼ m s^{-1}.

7. REFERENCES

Ament, W. S. 1953. "Toward a Theory of Reflection by a Rough Surface," *Proceedings of Institute of Radio Engineers,* vol. 41, pp. 142–146.

Barrick, D. E. 1998. "Grazing Behavior of Scatter and Propagation above Any Rough Surface," *IEEE Transactions on Antennas and Propagation,* vol. 46, pp. 73–83.

Cox, C. and W. Munk. 1954. "Measurement of the Roughness of the Sea Surface from Photographs of the Sun's Glitter," Journal of the Optical Society of America, vol. 44, pp. 838–850.

Cox, C. and W. Munk. 1955. "Some Problems in Optical Oceanography," Journal of Marine Research, vol. 14, pp. 63–78.

Cox, C. and W. Munk. 1956. "Slopes of the Sea Surface Deduced from Photographs of Sun Glitter," *Scripps Institute of Oceanography Bulletin 6,* pp. 401–487.

Hale, G. M. and M. R. Querry. 1973. "Optical Constants of Water in the 200 nm to 200 μm Wavelength Region," *Applied Optics,* vol. 12, pp. 555–563.

Kerr, D. E., W. T. Fishback, and H. Goldstein. 1951. *Propagation of Short Radio Waves,* pp. 411– 418, D. E. Kerr, Ed. McGraw-Hill, New York, NY.

Miller, A. R., R. M. Brown, and E. Vegh. 1984. "New Derivation for the Rough-Surface Reflection Coefficient and for the Distribution of Sea-Wave Elevations," *Institution of Electrical Engineers Proceedings,* vol. 131, pp. 114–116.

Minnaert, M. 1954. *Light and Color in the Open Air,* p. 23 ff. Dover, New York, NY.

Plass, G. N., G. W. Kattawar, and J. A. Guinn. 1975. "Radiative Transfer in the Earth's Atmosphere and Ocean: Influence of Ocean Waves," *Applied Optics,* vol. 14, pp. 1924–1936.

Shaw, J. A. 1999. "Glittering Light on Water," *Optics & Photonics News 10,* pp. 43–45, 68.

Stratton, J. A. 1941. *Electromagnetic Theory,* p. 505 ff. McGraw-Hill, New York, NY.

Querry, M. R., W. E. Holland, R. C. Waring, L. M. Earls, and M. D. Querry. 1977. "Relative Reflectance and Complex Refractive Index in the Infrared for Saline Environmental Waters," *Journal of Geophysical Research,* vol. 82, pp. 1425–1433 (Table 3, Pacific Ocean column).

Zeisse, C. R. 1995. "Radiance of the Ocean Horizon," *Journal of the Optical Society of America A,* vol. 12, pp. 2022–2030.

APPENDIX A
GRAZING AREA OF A ROUGH SURFACE

The fractional area of the rough ocean surface projected toward the receiver at any elevation is

$$\frac{B_r}{A} = \iint_{\substack{\omega \leq \pi/2 \\ U_r = const}} (\cos\omega / \cos\theta_n)\, p\, d\zeta_x d\zeta_y . \tag{A1}$$

The term in parentheses in the integrand of equation (A1) is

$$\begin{aligned}
\cos\omega / \cos\theta_n &= \mathbf{U}_r \cdot \mathbf{U}_n / \cos\theta_n \\
&= (a_r a_n + b_r b_n + c_r c_n)/c_n \\
&= -a_r \zeta_x - b_r \zeta_y + c_r \\
&= \cos\Psi_r \zeta_y + \sin\Psi_r
\end{aligned} \tag{A2}$$

where U_r and U_n point toward the receiver and along the facet normal, respectively, and a_r vanishes because the receiver is in the Y-Z plane.

The behavior of equation (A1) depends on whether or not the receiver observes from a grazing angle. In each case the key factor is the limit on the angle of incidence, ω.

Well away from grazing (for receiver elevations above about 10°), and for typical wind speeds, the limit on ω may be ignored. That is because under those conditions only the front sides of the facets will be presented to the receiver in the first place. After inserting (A2) into (A1), the trigonometric factors in (A2) may be brought outside the integral since they do not depend on facet slope. Using the facts that (1) p is even, (2) the slopes are odd, and (3) p is normalized to unity, it can be shown that the first term in (A2) vanishes during integration in (A1) and the second term in (A2) survives intact. Then the integral in (A1) is equal to sin Ψ_r, the value used by Cox and Munk.

At grazing (for receiver elevations below about 10°), the limit on ω may not be ignored. Furthermore, that limit, $\omega = \pi/2$, is equivalent to the condition $\zeta_y = -\tan\Psi_r$. Introducing these expressions and equation (A2) into equation (A1), and using the variables given in equation (10), the integral in (A1) becomes

$$\frac{B_r}{A} = \frac{1}{2\pi} \int_{-\infty}^{\infty} \exp(-u^2/2)\, du \int_{-v_o}^{\infty} (\cos\Psi_r \sigma v + \sin\Psi_r) \exp(-v^2/2)\, dv , \tag{A3}$$

where the absolute value of the reduced Y-slope limit is

$$v_o \equiv \tan\Psi_r / \sigma \geq 0 . \tag{A4}$$

This limit is small compared to one; it has a maximum of about 1/5 for the largest receiver angle of 10 mrad and the small wind speed of ¼ m s^{-1}. After carrying out the integration over u in equation (A3), the projected rough area at grazing becomes

$$\frac{B_r}{A} = \frac{\sigma}{\sqrt{2\pi}} \left\{ \cos \Psi_r I + \frac{\sin \Psi_r}{\sigma} J \right\}$$

$$I \equiv \int_{-v_o}^{\infty} v \exp(-v^2/2) dv \approx 1 - \frac{v_o^2}{2} - \frac{v_o^4}{8} \dots \qquad (A5)$$

$$J \equiv \int_{-v_o}^{\infty} \exp(-v^2/2) dv = \sqrt{\pi/2} \left\{ 1 + erf \left(v_o/\sqrt{2} \right) \right\}$$

Finally, I replace the trigonometric terms in equation (A5) with their small angle approximations, multiply, collect terms, and obtain the following expression for the fractional area of the ocean surface seen at the grazing angle, Ψ_r:

$$\frac{B_r}{A} \approx \frac{\sigma}{\sqrt{2\pi}} \left(1 + \sqrt{\frac{\pi}{2}} \ v_o + \frac{v_o^2}{2} - \frac{7}{24} v_o^4 + \dots \right) \equiv \frac{\sigma}{\sqrt{2\pi}} f(v_o) \qquad (A6)$$

$$v_o \approx \Psi_r/\sigma$$

REPORT DOCUMENTATION PAGE

Form Approved
OMB No. 0704-01-0188

1. REPORT DATE (DD-MM-YYYY)	2. REPORT TYPE	3. DATES COVERED (From - To)
10-2000	Technical	

4. TITLE AND SUBTITLE
GRAZING REFLECTIVITY OF THE WIND-RUFFLED SEA

5a. CONTRACT NUMBER

5b. GRANT NUMBER

5c. PROGRAM ELEMENT NUMBER
PE0602435N

6. AUTHORS
C. R. Zeisse

5d. PROJECT NUMBER

5e. TASK NUMBER
DN302215

5f. WORK UNIT NUMBER
MPB2

7. PERFORMING ORGANIZATION NAME(S) AND ADDRESS(ES)
SSC San Diego
San Diego, CA 92152-5001

8. PERFORMING ORGANIZATION REPORT NUMBER
TR 1843

9. SPONSORING/MONITORING AGENCY NAME(S) AND ADDRESS(ES)
Office of Naval Research
800 North Quincy Street
Arlington, VA 22217-5660

10. SPONSOR/MONITOR'S ACRONYM(S)
ONR

11. SPONSOR/MONITOR'S REPORT NUMBER(S)

12. DISTRIBUTION/AVAILABILITY STATEMENT
Approved for public release; distribution is unlimited.

13. SUPPLEMENTARY NOTES

14. ABSTRACT
This report provides a formula derived for the grazing optical reflectivity of an ocean covered by capillary waves. The formula applies to circular sources such as the Sun.

15. SUBJECT TERMS
Mission Area: Command, Control, Communications
atmospheric physics
propagation assessment
environmental data
reflectivity

16. SECURITY CLASSIFICATION OF:			17. LIMITATION OF ABSTRACT	18. NUMBER OF PAGES	19a. NAME OF RESPONSIBLE PERSON
a. REPORT	b. ABSTRACT	c. THIS PAGE			C. R. Zeisse
U	U	U	UU	38	19B. TELEPHONE NUMBER (Include area code) (619) 553-3602

Standard Form 298 (Rev. 8/98)
Prescribed by ANSI Std. Z39.18

INITIAL DISTRIBUTION